Crystalline thin films of β-phase poly(9,9-dioctylfluorene)

Takuji Kawamura, Masahiro Misaki, Yasuko Koshiba, Satoshi Horie, Kenji Kinashi, Kenji Ishida, Yasukiyo Ueda *

Graduate School of Engineering, Kobe University, 1-1 Rokko, Nada, Kobe 657-8501, Japan

ABSTRACT

The detailed structure of crystalline β-phase poly(9,9-dioctylfluorene) (PFO) films was studied by polarized optical measurements, transmission electron microscopy, and grazing-incidence X-ray diffraction. Crystalline β-phase PFO thin films were fabricated by a friction transfer technique and subsequent vapor treatment. Compared to the α-phase, the lattice parameters of the β-phase crystals shrank along the a-axis (film thickness direction) and elongated along the b-axis (side-chain direction), but the period along the c-axis (main-chain direction) remained nearly equal. These changes in molecular packing were consistent with a planar conformational change from the α-phase to the β-phase of PFO.

© 2010 Elsevier B.V. All rights reserved.

1. Introduction

Polyfluorenes (PFs) have emerged as an attractive semiconducting polymer material for light-emitting diodes (LEDs), field-effect transistors (FETs), and photovoltaic cells due to their excellent electrical and optical properties, reasonable chemical stability, and ease of processability [1–3]. PFs exhibit thermal liquid crystallinity, leading to the alignment of polymer chains after annealing on rubbed substrates [4]. Among PFs, poly(9,9-dioctylfluorene) (PFO) has attracted much attention as a standard PF material and a pure blue-emitting polymer.

PFO exhibits three solid-state phases at room temperature: the nematic (N)-phase, the α-phase, and the β-phase [5]. PFO films containing N-phase and α-phase can be obtained, depending on the cooling rate from 463 K (nematic liquid crystal state) to room temperature; rapid quenching and slow cooling result in N-phase and α-phase, respectively. On the other hand, generation of the β-phase usually requires additional treatment, such as cooling to 80 K and then reheating to room temperature or exposure to certain solvent vapors [6]. However, some freshly prepared films can contain significant amounts of the β-phase without any additional treatment [7].

The β-phase of PFO forms a more planar conformation than the α- or N-phases, and also has significantly different photophysical properties. β-Phase PFO has a distinctive UV-Vis absorption peak at 433 nm, and a red-shifted photoluminescence (PL) spectrum [8]. Many spectroscopic studies of β-phase PFO have been reported [9,10], but only a few structural studies have been carried out [11]. In the latter research, Chen et al. reported structural and morphological features of the β-phase, and defined it as a noncrystalline phase [12]. However, no correlation between molecular conformation and packing has yet been established.

We previously reported that the efficiency of LEDs based on β-phase PFO reached 2.0 cd/A, which is twice that of LEDs based on the other phases [2]. However, the detailed mechanism of this high efficiency remains unclear. In this study, we investigated the film structure of β-phase PFO using polarized optical spectroscopy, transmission electron microscopy (TEM), and grazing-incidence X-ray diffraction (GIXRD), and will discuss the structural basis of the high LED efficiency.

2. Experiment

The PFO used in this study was purchased from American Dye Source, Inc. (cat. No. ADS129BE). The number- and weight-average molecular weights, as determined by gel permeation chromatography (GPC, Shimadzu LC-10Vp HPLC System) with a TOSOH G5000HHR GPC column calibrated using a polystyrene standard, were $M_n = 25000$ and $M_w = 55000$ (polydispersity $= 2.2$), respectively. Uniaxially oriented films of PFO were prepared on glass and silicon substrates b.y a friction transfer technique, which is a simple process that does not involve volatile organic compounds (VOCs) [4]. The

friction transfer process was carried out by squeezing and drawing a PFO pellet on a substrate maintained at 383 K. The applied squeezing load was 4.1 kgf/cm^2, and the drawing speed was 0.5 m/min. In order to obtain the β-phase, the friction-transferred films were exposed to saturated toluene vapor for approximately 100 h.

Since our evaluation methods were previously described in detail [4], only a brief outline is given here. The optical properties of the films were characterized using an ultraviolet-visible (UV-Vis) absorption spectrometer (JASCO V-670) and a fluorescence spectrometer (HITACHI F-2500). The polarization dependence was analyzed using a Glan-Thompson prism. For structural analysis, the films were observed by TEM (HITACHI H-7100). The transmission electron micrographs and the electron diffraction (ED) patterns were recorded at an acceleration voltage of 100 kV. For GIXRD, we used the BL13XU beam line of SPring-8 (Japan Synchrotron Radiation Research Institute (JASRI), Hyogo, Japan) equipped with an ATX-GSOR of the ATX series from Rigaku Co. The wavelength λ was 0.1 nm and the grazing angle of incidence ω was fixed at 0.14°. A Soller slit with a divergence angle of 0.45° was placed in front of the detector. In this study, the out-of-plane structure was investigated by GIXRD, where 2θ was scanned and the scattering vector Q_{out} was defined as $4\pi\sin\theta/\lambda$.

3. Results and discussion

Fig. 1(a) shows polarized UV-Vis absorption spectra of friction-transferred films before and after vapor treatment. Here, we defined the absorption spectra parallel and perpendicular to the friction direction as $A_{//}$ and $A_\perp$, respectively. $A_{//}$ before vapor treatment (described as before $A_{//}$) had a major absorption maximum at 397 nm, which was associated with π−π* transitions [4]. On the other hand, $A_{//}$ after vapor treatment (described as after $A_{//}$) clearly had an additional

Fig. 1. Polarized (a) UV-Vis absorption and (b) PL spectra of friction-transferred films, before and after vapor treatment.

absorption peak at 433 nm, which was unique to the β-phase. However, for $A_\perp$ after vapor treatment (described as after $A_\perp$), the absorption intensity was sufficiently suppressed. The dichroic ratio of absorption (after $A_{//}$ / after $A_\perp$) was approximately 9.4 at 400 nm, indicating that the β-phase PFO chains were aligned highly parallel to the friction direction.

The in-plane anisotropy of films can also be determined from their polarized PL spectra. Fig. 1(b) shows polarized PL spectra of friction-transferred films before and after vapor treatment. In these PL spectra, we defined the parallel and perpendicular components with respect to the friction direction as I_{zz} and I_{zx}, respectively. The excitation wavelength was 380 nm. I_{zz} before vapor treatment (described as before I_{zz}) showed a well-resolved vibronic progression, with peaks at 437, 462, and 493 nm. On the other hand, I_{zz} after vapor treatment (described as after $I_{//}$) had a red-shifted emission compared with before I_{zz}, and a vibronic structure with peaks at 442, 468, and 500 nm, which were unique to the β-phase. However, these peaks were significantly suppressed in I_{zx} after vapor treatment (described as after I_{zx}). The dichroic ratio of PL (after I_{zz} / after I_{zx}) was estimated to be 5.0 at 442 nm. Thus, the friction-transferred PFO film with vapor treatment exhibited a remarkable dichroism of its optical properties.

The in-plane structure of the films was studied using TEM observation. Fig. 2(a) shows a TEM image and ED pattern of a film before vapor treatment. Here, we note that the friction direction was always vertical, and the inserted white curve indicates the profile intensity at the equator. Diffraction spots were clearly observed at a spacing of 0.561 and 0.419 nm along the meridian and 0.597 and 0.399 nm along the equator, which were assigned to 006, 008, 040, and 060 reflections, respectively, of the α-phase crystal (orthorhombic, $a = 2.56$ nm, $b = 2.34$ nm, $c = 3.32$ nm). This indicated that the main-chains (c-axis) and alkyl side-chains (b-axis) were oriented parallel and orthogonal to the friction direction, respectively. The TEM image showed long grains of α-phase crystal with a preferred orientation parallel to the friction direction. Fig. 2(b) shows, on the other hand, a TEM image and ED pattern of a film after vapor treatment, which was identified as a β-phase film by UV-Vis absorption and PL spectra. Strong diffraction spots were observed at a spacing of 0.420 nm on the meridian, which was almost same as that observed before vapor treatment. However, the profile on the equator was clearly different from that of the film before vapor treatment; the diffuse diffraction spots, corresponding to spacings of 0.663 and 0.448 nm (indicated by arrows) were observed. Here, it should be noted that β-phase PFO exists as a crystal, at least in the range of the TEM observations, and the conformational change from α-phase to β-phase clearly affected its molecular packing. The estimated lattice parameters of the β-phase crystal are summarized in Table 1. The b-axis (side-chain direction) lattice parameter of the β-phase crystal was up to 11.3% larger than that of α-phase crystal. This elongation along the b-axis suggests a conformational change from the α-phase to β-phase of PFO resulted in a more planar arrangement, in which alkyl side-chains located in the same plane as fluorene units hindered close packing of the PFO along the b-axis. Although dramatic changes appeared in the ED patterns, the TEM images remained unchanged.

Fig. 3 shows GIXRD patterns from films before and after vapor treatment. The film before vapor treatment (solid line) had a peak at $Q_{out} = 5.0$ nm^{-1} ($d = 1.25$ nm) corresponding to the 200 reflection of the α-phase crystal [12]. On the other hand, the film after vapor treatment (dashed line) had a peak at $Q_{out} = 5.3$ nm^{-1} ($d = 1.19$ nm), indicating that the lattice spacing of β-phase contracted along the a-axis (film thickness direction). The shrinkage along the a-axis can be explained by assuming a conformational change from the α-phase to the β-phase: a more planar conformation enabled the PFO to pack more closely along the a-axis. Since the π-stacking direction of PFO is parallel to the a-axis, this shrinkage induces stronger intermolecular interaction.

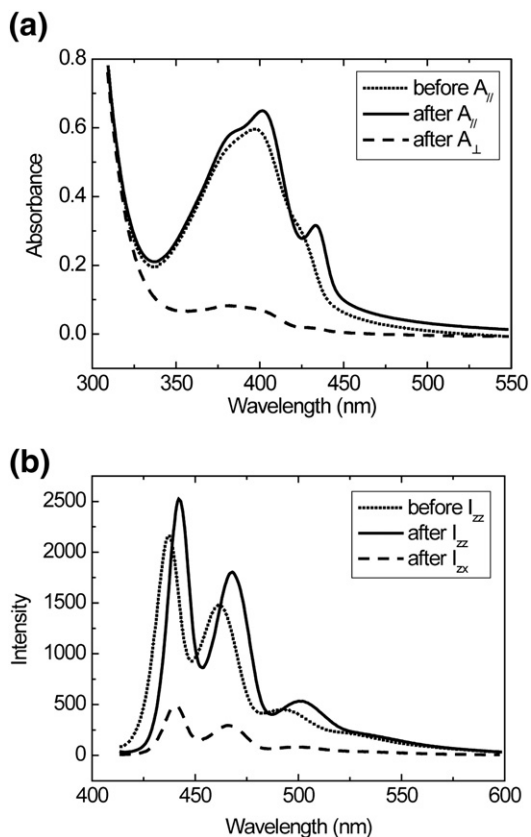We have attempted to measure the hole mobility of the PFO friction-transferred films. But it was difficult to measure the hole